LA-UR- 09-05208

Approved for public release; distribution is unlimited.

Title: An Exact Solution for the History-Dependent Material and Delamination Behavior of Laminated Plates Subjected to Cylindrical Bending.

Author(s): Todd O. Williams T-3

Intended for: AIAA SDM Conference
Orlando, FL
April 14-16, 2010

Los Alamos
NATIONAL LABORATORY
EST. 1943

An Exact Solution for the History-Dependent Material and Delamination Behavior of Laminated Plates Subjected to Cylindrical Bending

Todd O. Williams*

Los Alamos National Laboratory, Los Alamos, New Mexico, 87545, USA

The exact solution for the history-dependent behavior of laminated plates subjected to cylindrical bending is presented. The solution represents the extension of Pagano's solution[1] to consider arbitrary types of constitutive behaviors for the individual lamina as well as arbitrary types of cohesive zones models for delamination behavior. Examples of the possible types of material behavior are plasticity, viscoelasticity, viscoplasticity, and damaging. Examples of possible CZMs that can be considered are linear, nonlinear hardening, as well as nonlinear with softening. The resulting solution is intended as a benchmark solution for considering the predictive capabilities of different plate theories.

Initial results are presented for several types of history-dependent material behaviors. It is shown that the plate response in the presence of history-dependent behaviors can differ dramatically from the elastic response. These results have strong implications for what constitutes an appropriate plate theory for modeling such behaviors.

Keywords: Laminated plates, elasticity, exact solution, history-dependent material response, delamination, cohesive zone model

I. Introduction

As composite structures become increasingly common as major load bearing structures it becomes ever more important to develop accurate predictive models for their behaviors. Since such structures must often operate in the regimes dominated by both history-dependent material responses as well as delamination damage a predictive plate theory must be able to consider these phenomena. The types of history-dependent materials behaviors possible with a given laminated structure can cover a broad range of response characteristics depending on the types of lamina present in the structure. Examples of possible material behaviors include plasticity, viscoelasticity, viscoplasticity, and damage/strain softening responses. The possible delamination responses exhibit a similarly broad range of possibilities.

Given the general characteristics of such laminated structures, plate theories are often used to model the structural response. There are a wide variety of possible theories ranging from simple classical lamination theory to discrete layer theories[2] to multiscale theories.[1-6] The vast majority of these plate theories have been developed with the (often implicit) assumptions of linear material behavior and perfect bonding. Those that consider delamination restrict attention to a linear model for delamination behavior which is only appropriate for initiation and preliminary growth. It is often unclear whether a given type of established plate theory is even capable of predicting the behaviors of laminated structures in the presence of history-dependent material and delamination responses.

*Technical Staff Member, Theoretical Division, T-3, MS B216, Los Alamos NM 87545.

In reality both history-dependent material behaviors and delamination initiation and growth behaviors are nonlinear processes. Therefore, in order to achieve predictive capabilities a given theory must be able to accurately predict the pointwise fields in order to correctly predict these nonlinear evolutionary processes.

Exact benchmark solutions are an essential ingredient for determing whether a given plate theory has the appropriate predictive capabilities. Currently all such exact solutions that the author is aware of are for elastic material behavior and linear delamination behavior. The current work presents the development of an exact solution for cylindrical bending of laminated plates in the presence of arbitrary history-dependent material and delamination behavior. Results are presented for a number of different lamination schemes and material behaviors. This initial work is restricted to perfectly bonded laminates. These results show that the introduction of history-dependent material responses causes the local and global responses of the plate to continually diverge from the elastic response. Furthermore, these results show that many current used plate theories may be inadequate for predicting the history-dependent response of laminated plates.

II. General Formulation

The following solution is developed using a displacement formulation for the governing equations of elasticity. The solution is given in terms of general Fourier series expansions for the different fields.

Consider a simply-supported, infinite strip, laminated plate composed of an arbitrary number of layers N. A layer can consist of a single lamina or of a subregion of a lamina. The lamina may be either perfectly bonded or have displacement jumps across the interfaces due to delamination. The transverse coordinate is denoted by x_3 while the inplane coordinate is denoted by x_1. Given the infinite strip nature of the problem there is no dependence on the out-of-plane coordinate x_2.

The following conventions are used throughout the formulation. Superscripts '(k)' denote the layer number where $k = 1, ..., N$. Both total and indicial notation is used in the development. The number of underlines under a term indicates the matrix order of the term. Latin indices have a range of 1 to 3 while Greek indices have a range of 1 to 2. Summation is implied on repeated Latin and Greek indices. A prime denotes partial differentiation with respect to the spatial coordinates. The order of a term in an expansion is denoted by (n) and summation on repeated order indices is assumed. The bottom and top surfaces of a layer are denoted by x_3^{k-1} and x_3^k, respectively.

A sufficiently general form of the geometrically linear, history-dependent constitutive relations for material behavior at a point within a given lamina is given by

$$\sigma_{ij} = C_{ijkl}\epsilon_{kl} + \lambda_{ij} \tag{2.1}$$

where the σ_{ij} are the stress tensor components, the C_{ijkl} are the elastic stiffness tensor components where the greatest degree of anisotropy is monoclinic about the x_3 axis, the ϵ_{kl} are the geometrically linear strain tensor components, and the λ_{ij} are the eigenstress components. All of the history-dependent effects are incorporated in the eigenstresses λ_{ij}. These history-dependent effects can have any type of evolutionary process and thus all types of history-dependent constitutive relations can be cast in this form.

Consistent with Pagano,[1] the displacement field within the k^{th} layer is given by

$$u_\alpha(x,t) = U_{\alpha.(n)}(x_3,t)\,cos\left(p_{(n)}x_1\right) \quad , \quad u_3(x,t) = U_{3.(n)}(x_3,t)\,sin\left(p_{(n)}x_1\right) \tag{2.2}$$

where $p_{(n)} = n\pi/L$, $n = 1, 2, 3...$, and L is the width of the plate.

The corresponding strain field within the lamina is

$$\epsilon_{11} = -p_{(n)}U_{1(n)}sin\left(p_{(n)}x_1\right) \quad , \quad \epsilon_{22} = 0 \quad , \quad \epsilon_{33} = U'_{3(n)}sin\left(p_{(n)}x_1\right)$$
$$\epsilon_{23} = \frac{1}{2}U'_{2(n)}cos\left(p_{(n)}x_1\right) \quad , \quad \epsilon_{13} = \frac{1}{2}\left(U'_{1(n)} + p_{(n)}U_{3(n)}\right)cos\left(p_{(n)}x_1\right) \quad , \quad \epsilon_{12} = -\frac{1}{2}p_{(n)}U_{2(n)}sin\left(p_{(n)}x_1\right) \tag{2.3}$$

Based on these forms for the strains the eigenstrains are expanded according to the same forms, i.e.

$$\lambda_{11} = \eta_{11(n)} sin\left(p_{(n)}x_1\right) \quad , \quad \lambda_{22} = \eta_{22(n)} sin\left(p_{(n)}x_1\right) \quad , \quad \lambda_{33} = \eta_{33(n)} sin\left(p_{(n)}x_1\right)$$
$$\lambda_{23} = \eta_{23(n)} cos\left(p_{(n)}x_1\right) \quad , \quad \lambda_{13} = \eta_{13(n)} cos\left(p_{(n)}x_1\right) \quad , \quad \lambda_{12} = \eta_{12(n)} sin\left(p_{(n)}x_1\right) \tag{2.4}$$

where the usual rules of Fourier analysis apply for determining the magnitues $\eta_{ij(n)}$. Symmetry holds for the strain, stress, and eigenstress fields.

Substituting the above fields into the equations of equilibrium and using the orthogonality properties of the trig functions gives the following forms for the equilibrium equations for each harmonic in the expansions for each layer

$$-p_{(n)}^2 C_{1111} U_{1(n)} + C_{1313} U''_{1(n)} - p_{(n)}^2 C_{1112} U_{2(n)} + C_{1323} U''_{2(n)} + p_{(n)} \left(C_{1133} + C_{1313}\right) U'_{3(n)}$$
$$+ p_{(n)} \eta_{11(n)} + \eta'_{13(n)} = 0 \tag{2.5a}$$

$$-p_{(n)}^2 C_{1211} U_{1(n)} + C_{2313} U''_{1(n)} - p_{(n)}^2 C_{1212} U_{2(n)} + C_{2323} U''_{2(n)} + p_{(n)} \left(C_{1233} + C_{2313}\right) U'_{3(n)}$$
$$+ p_{(n)} \eta_{12(n)} + \eta'_{23(n)} = 0 \tag{2.5b}$$

$$-p_{(n)} \left(C_{1313} + C_{3311}\right) U'_{1(n)} - p_{(n)} \left(C_{1323} + C_{3312}\right) U'_{2(n)} - p_{(n)}^2 C_{1313} U_{3(n)} + C_{3333} U''_{3(n)}$$
$$- p_{(n)} \eta_{13(n)} + \eta'_{33(n)} = 0 \tag{2.5c}$$

This system of governing equations can be converted into a system of first order ODEs using standard techniques. The resulting system of governing equations is given by

$$\underline{X}' + \underline{\underline{c}}\,\underline{X} + \underline{f} = 0 \tag{2.6}$$

where $\underline{X} = \left(U_{1(n)}, U_{2(n)}, U_{3(n)}, Y_{1(n)}, Y_{2(n)}, Y_{3(n)}\right)^T$ where $Y_{i(n)} = U'_{i(n)}$; $\underline{\underline{c}}$ is a known coefficent matrix that is a function of $p_{(n)} = n\pi/L$ and the stiffness tensor C for a given lamina, and $\underline{f}$ is a function of the eigenfield and its gradients, the stiffness tensor C, and $p_{(n)} = n\pi/L$. The solution of this system of governing equations (based on the solution form $\underline{X} = \underline{\chi} e^{sx_3}$) results in an eigenvalue problem with a sixth order characteristic equation in the eigenvalues s. Using standard techniques this sixth order equation can be reduced to cubic characteristic equation of the form

$$\gamma^3 + a\gamma + b = 0 \tag{2.7a}$$

which can be solved analytically. The associated equations for determining the eigenvectors are of the form

$$\left(\underline{\underline{c}} + s\underline{\underline{I}}\right)\underline{\chi} = 0 \tag{2.7b}$$

where $\underline{\underline{I}}$ is the identity matrix and s is a function of γ. Depending on the properties of the transformations used to obtain Eqn. 2.7 and its coefficients the eigenvalues, s, can be complex or real.

Based on classical solution techniques the particular solution of the governing equations for each harmonic in each layer is given by

$$\underline{X}_{(n)} = \underline{\underline{\Psi}}_{(n)} \underline{d}_{(n)} - \underline{\underline{\Psi}}_{(n)} \int_{x_3^{k-1}}^{x_3^k} \underline{\underline{\Psi}}_{(n)}^{-1} \underline{f}_{(n)} ds = \underline{\underline{\Psi}}_{(n)} \left(\underline{d}_{(n)} - \underline{I}_{(n)}\right) \tag{2.8}$$

where $\underline{\underline{\Psi}}_{(n)}$ is the fundamental matrix of the homogeneous solution and $\underline{d}_{(n)}$ is a coefficient matrix to be determined from the interfacial constraints and the top and bottom surface boundary conditions. Note that $\underline{I}_{(n)}$ is a vector term associated with the integral effects for order n in the expansions and is not the identity matrix. It is noted that the history-dependent responses due to material behavior is incorporated into the term $\underline{f}$. It is useful to note that the fundamental matrix can be expressed in the form $\underline{\underline{\Psi}}_{(n)} = \underline{\underline{H}}_{(n)} \underline{\underline{\beta}}_{(n)}$ where $\underline{\underline{H}}_{(n)}$ is, in general, a fully populated constant matrix and $\underline{\underline{\beta}}_{(n)}$ is a sparse matrix that is a function of x_3. The inversion of the fundamental matrix is carried out using $\underline{\underline{\Psi}}^{-1}_{(n)} = \underline{\underline{\beta}}^{-1}_{(n)} \underline{\underline{H}}^{-1}_{(n)}$ where $\underline{\underline{H}}^{-1}_{(n)}$ is determined numerically and $\underline{\underline{\beta}}^{-1}_{(n)}$ is determined analytically. This functional separation of $\underline{\underline{\Psi}}_{(n)}$ is useful for evaluating the integral terms in Eqn. 2.8.

Based on the above solution forms, the displacement field within a layer is given by

$$u_{\alpha}^{(k)} = \left(\Psi_{(n)\alpha j} \left(d_{(n)j} - I_{(n)j}\right)\right) cos\left(p_{(n)} x_3\right)$$
$$u_{3}^{(k)} = \left(\Psi_{(n)3j} \left(d_{(n)j} - I_{(n)j}\right)\right) sin\left(p_{(n)} x_3\right) \tag{2.9}$$

Note that summation over the harmonic order n is assumed. The corresponding strain and stress fields within each layer can be directly determined from Eqn. 2.9 using the strain-displacement relations and the constitutive relations.

As mentioned above, the unknown constant vectors for each harmonic in each layer are determined from the interfacial constraints and the top and bottom surface boundary conditions. In particular, the interfacial constraints used to determine these constants take the forms

$$\sigma_{i3(n)}^{(k+1)}\left(x_3^{(k)}, t\right) - \sigma_{i3(n)}^{(k)}\left(x_3^{(k)}, t\right) = 0 \qquad k = 1, ..., N-1 \tag{2.10a}$$

$$u_{i(n)}^{(k+1)}\left(x_3^{(k)}, t\right) - u_{i(n)}^{(k)}\left(x_3^{(k)}, t\right) = f^{(k)}\left(\sigma_{i3}^{(k)}, \mu^{(k)}, t\right) \qquad k = 1, ..., N-1 \tag{2.10b}$$

where $f^{(k)}\left(\sigma_{i3}, \mu, t\right)$ is a some arbitrary cohesive zone model (CZM) which depends on the interfacial stress state given by $\sigma_{i3}^{(k)}$ and some general set of internal state variables for the CZM which is denoted by $\mu^{(k)}$. The boundary conditions at the top surface take one of the forms

$$u_{i(n)}^{(N)}\left(x_3^{(N)}, t\right) = u_{i(n)}^{BC}(t) \tag{2.11a}$$

or

$$\sigma_{i3(n)}^{(N)}\left(x_3^{(N)}, t\right) = \sigma_{i3(n)}^{BC}(t) \tag{2.11b}$$

where $u_{i(n)}^{BC}(t)$ and $\sigma_{i3(n)}^{BC}(t)$ are the specified boundary condition. Similar relations hold for the boundary conditions at the bottom of the plate.

Substituting the expressions for the stress and displacement fields into the the interfacial constraints, Eqn. 2.10, and the top/bottom surface boundary conditions, Eqn. 2.11, gives a final system of equations of the form

$$\underline{D} = \underline{\underline{\Delta}} \underline{F} \tag{2.12}$$

to be solved for the unknown global vector of unknowns $\underline{D}$ which is composed of the individual unknown vectors $\underline{d}_{(n)}^{(k)}$. The global coefficient matrix $\underline{\underline{\Delta}}$ is a known function of the harmonics, the material properties for the different layers, and the geometric properties of the layers. The global forcing vector $\underline{F}$ is a function of the CZMs at the different interfaces and the applied boundary conditions at the top and bottom surfaces of the plate as well as the geometric and stiffness properties of the different layers.

III. Results

Some preliminary results for a bilaminate of aspect ratio of 10 composed of a plastically deforming aluminum (AL) top layer and an elastic graphite/epoxy (Gr/Ep) bottom layer are presented. The fibers in the Gr/Ep layer are oriented along the x_1 axis. The aluminum properties are given by a Young's modulus of $E = 72.4$ GPa, a Poisson's ratio of $\nu = 0.33$, a yield stress of $\sigma^Y = 286.67$ GPa, and a hardening slope of $H = 23.428$ GPa. The Gr/Ep layer has effective properties given by $E_{11} = 25.0$ GPa, $E_{22} = E_{33} = 1.0$ GPa, $\nu_{23} = \nu_{13} = \nu_{12} = 0.25$, $G_{23} = 0.2$ GPa, and $G_{13} = G_{12} = 0.5$ GPa.

The laminate is subjected to a normal monotonic loading with a single sine harmonic with a magnitude of 10 MPa. All results for this example are presented at the peak loading state. The analysis is carried out using 80 harmonics for the responses of each layers. The inelastic response due to plasticity is calculated on a mesh in the aluminum layer of 101 points in the x_1 direction and 50 points in the x_3 direction. An iterative response scheme is used to ensure convergence of the plastic field and thus the local and global responses. The iterative process was carried out until an error tolerance of 10^{-3} for the difference in the effective plastic strains between iterates at every point in the mesh was achieved. The details of the plasticity implementation are given by Williams and Pindera.[3]

The results are presented in terms of the following nondimensionalizations

$$u_1^*(0,x_3) = \frac{E_t u_1(0,x_3)}{q_1 h S^3} \quad u_3^*(L/2,x_3) = \frac{100 E_t u_3(L/2,x_3)}{q_1 h S^4}$$
$$\sigma_{11}^*(L/2,x_3) = \frac{\sigma_{11}(L/2,x_3)}{q_1 S^2} \quad \sigma_{22}^*(L/2,x_3) = \frac{\sigma_{22}(L/2,x_3)}{q_1 S^2} \quad \sigma_{33}^*(L/2,x_3) = \frac{\sigma_{33}(L/2,x_3)}{q_1 S^2}$$
$$\sigma_{23}^*(0,x_3) = \frac{\sigma_{13}(0,x_3)}{q_1 S^2} \quad \sigma_{13}^*(0,x_3) = \frac{\sigma_{13}(0,x_3)}{q_1 S^2} \quad \sigma_{12}^*(L/2,x_3) = \frac{\sigma_{12}(L/2,x_3)}{q_1 S^2} \tag{4.2.3}$$
$$S = \frac{L}{h} \quad x_3^* = \frac{x_3}{h} \quad x_1^* = \frac{x_1}{L}$$

where $q_1 = 10.0$ MPa and the plate has an aspect ratio of $S = 10$. The Young's modulus used to normalize the results is $E_t = 1.0$ GPa. The differences in the fields are given by the difference between the plastic and elastic fields divided by the elastic field.

The distributions through the thickness of the plate for the inplane displacement u_1^* and transverse displacement u_3^* are presented in Figures 1 and 2, respectively. The greatest difference between the elastic and plastic responses for u_1^* occurs at the top of the plate and exhibits a 19.55% difference between the elastic and plastic plates. The effect of plasticity on this displacement component is to cause the displacement value away from the midplane to increasingly diverge from the elastic response. Thus the maximum divergences occur at the top and both surfaces. It is worth noting that the variation in this component of the displacement field can not be adequately represented by a single kinematic representation. The maximum difference in u_3^* occurs at $x_3^* = 0.163$ and is 14.33%. The overall trends in the distribution of this field are similar for both the elastic and plastic responses and thus the primary effect of plasticity is to shift this displacement component to a higher value.

The distributions through the thickness of the stresses σ_{11}^*, σ_{33}^*, and σ_{13}^* are given in Figures 3-5, respectively. The response of σ_{11}^* in the presence of plasticity shows some rather strong deviations from the elastic behavior. In particular, there are several abrupt changes in the slopes of this stress component in the plastically deforming Al layer. These kinks correspond to the presence of edges of the plastic deformation zones. Most of the plastic deformation is at this point occurring in the top part of the layer although some plasticity is also starting to occur at the interface between the layers. The largest deviation between the elastic and plastic responses occurs at the top of the laminate and is 11.79%. The overall impact of the plasticity is to increase the stress state in the lower 3/4 of the Al layer while decreasing it in the top of this layer. The overall effect in the Gr/Ep layer is to decrease the magnitude of the stresses. One implication of this is that if loading were to continue then the Al layer would be required to accept increasing amounts

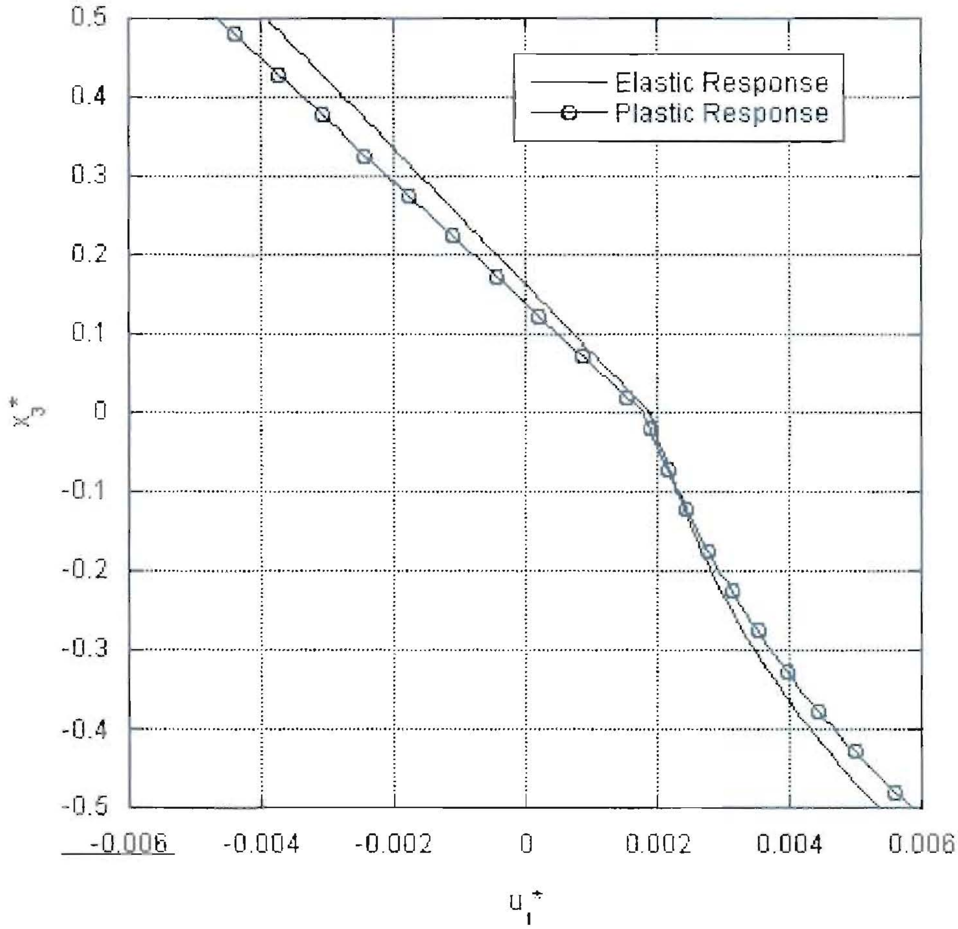

Figure 1. Distribution of u_1^* through the thickness of the plate for both elastic and plastic responses.

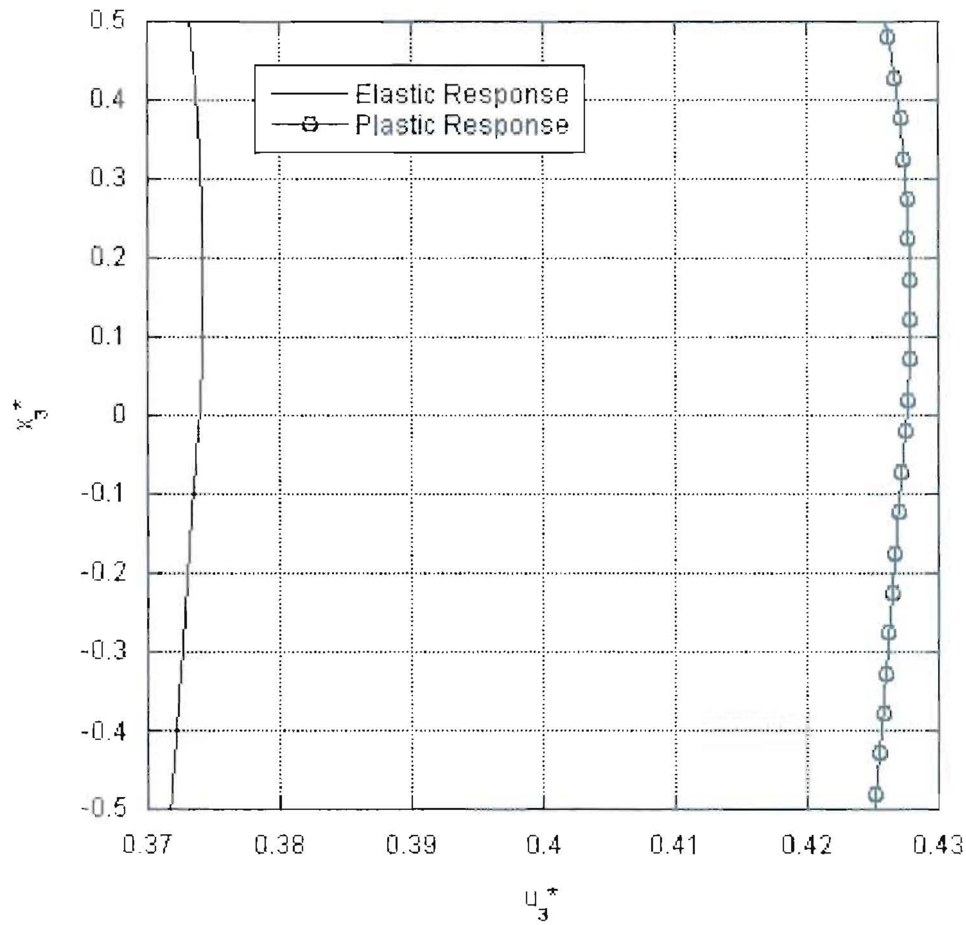

Figure 2. Distribution of u_3^* through the thickness of the plate for both elastic and plastic responses.

of the loading and thus would exhibit increasing amounts of plastic deformations. Consideration of the σ^*_{33} response, Fig. 4, shows that the effect of plasticity is to increase the magnitude of the stress at any given location through the thickness of the plate except for the top and bottom surfaces where the values must correspond due to the imposed boundary conditions. The maximum deviation between the elastic and plastic responses for σ^*_{33} occurs just slightly above the midplane and has a magnitude of 17%. The increase in σ^*_{33} at the interface between the two layers has implications for delamination initiation and growth; in particular, the increase would make delamination initiation more likely. Consideration of the σ^*_{13} through the thickness of the plate shows that plasticity has a less significant impact on this field than for the previous stresses. The peak value of the stress, which occurs in the Al layer, decreases by 1.94%. The overall effect in the Gr/Ep layer is to increase the magnitude of the stress slightly.

IV. Conclusions

An exact solution for the history-dependent response of a laminate in cylindrical bending has been presented. The solution is sufficiently general that any type of history-dependent material response within the geometrically linear response regime can be considered. Additionally, the solution accounts for delamination behaviors through the use of arbitary CZMs. It is intended that the solution be used as a benchmark solution for considering the suitability of different plate theories for application to structures undergoing history-dependent deformations.

It has been shown, using the example of a plastically deforming bilaminate, that plasticity can significantly effect the pointwise field variations within the laminate.

Acknowlegdements

This work was carried out under the auspices of the National Nuclear Security Administration of the U.S. Department of Energy at Los Alamos National Laboratory under Contract No. DE-AC52-06NA25396 as well as the Joint DOE and Department of Defense (DoD) Munitions Technology Development Program.

References

[1] Pagano, N., "Exact Solutions for Composite Laminates in Cylindrical Bending," *J. Comp. Mat.*, Vol. 3, 1969, p. 398.

[2] Reddy, J.N., "Mechanics of Laminated Composite Plates and Shells: Theory and Analysis,", CRC Press, Boca Raton, USA.

[3] Williams, T. O. and Pinder, M.-J. "An Analytical Model for the Inelastic Axial Shear Response of Unidirectional Metal Matrix Composites," *Int. J. Plast.*, Vol. 13, No. 3, 1997, pp. 261-289

[4] Williams, T. O., "A Generalized Multilength Scale Nonlinear Composite Plate Theory with Delamination," *Int. J. Solids Struct.*, Vol. 36, 1999, pp. 3015–3050.

[5] Williams, T. O., "A Generalized, Multilength Scale Framework for Thermo-Diffusionally-Mechanically Coupled, Nonlinear, Laminated Plate Theories with Delaminations," *Int. J. Solids Struct.*, Vol. 42, 2005, pp. 1465–1490.

[6] Williams, T. O., "A New Theoretical Framework for the Formulation of General, Nonlinear, Multi-Scale Plate Theories", Vol. 45, No. 9, 2008, pp. 2534-2560.

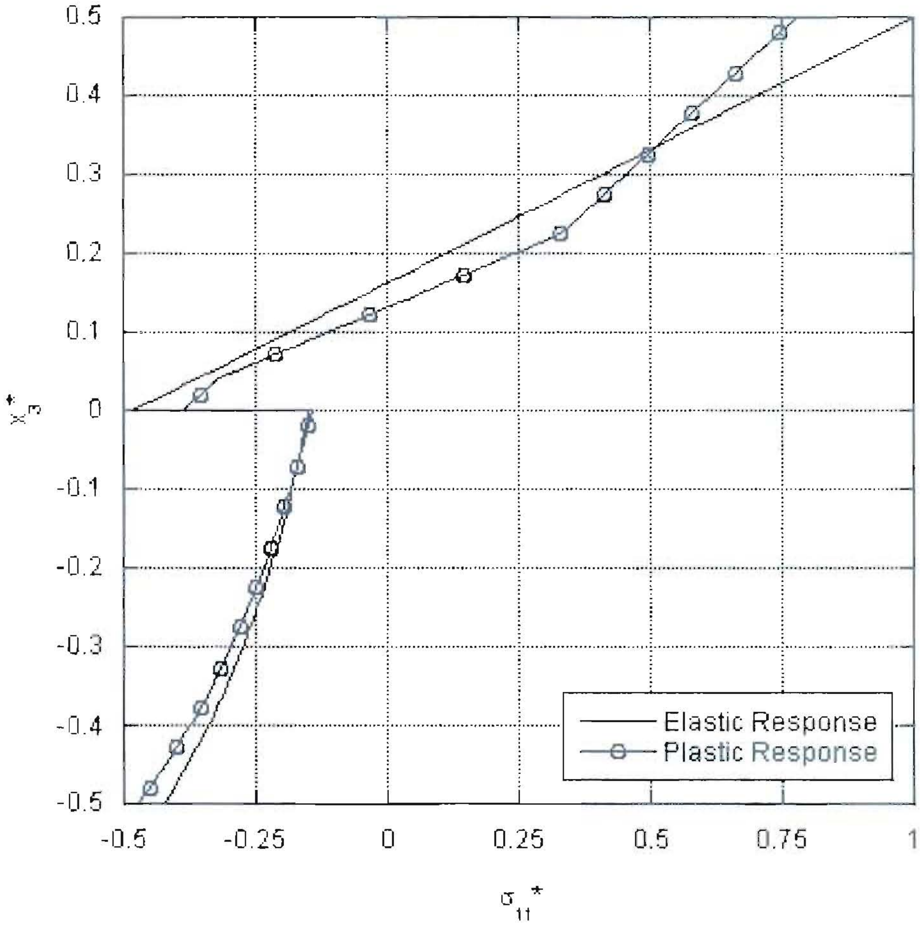

Figure 3. Distribution of σ^*_{11} through the thickness of the plate for both elastic and plastic responses.

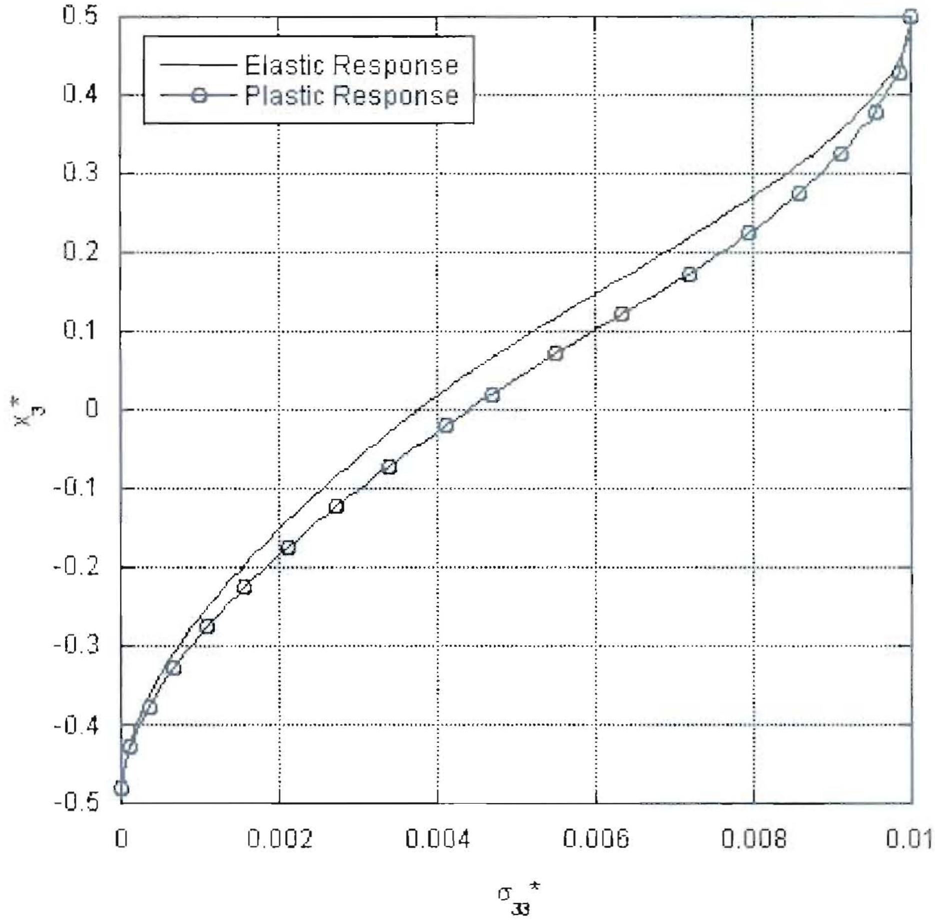

Figure 4. Distribution of σ_{33}^* through the thickness of the plate for both elastic and plastic responses.

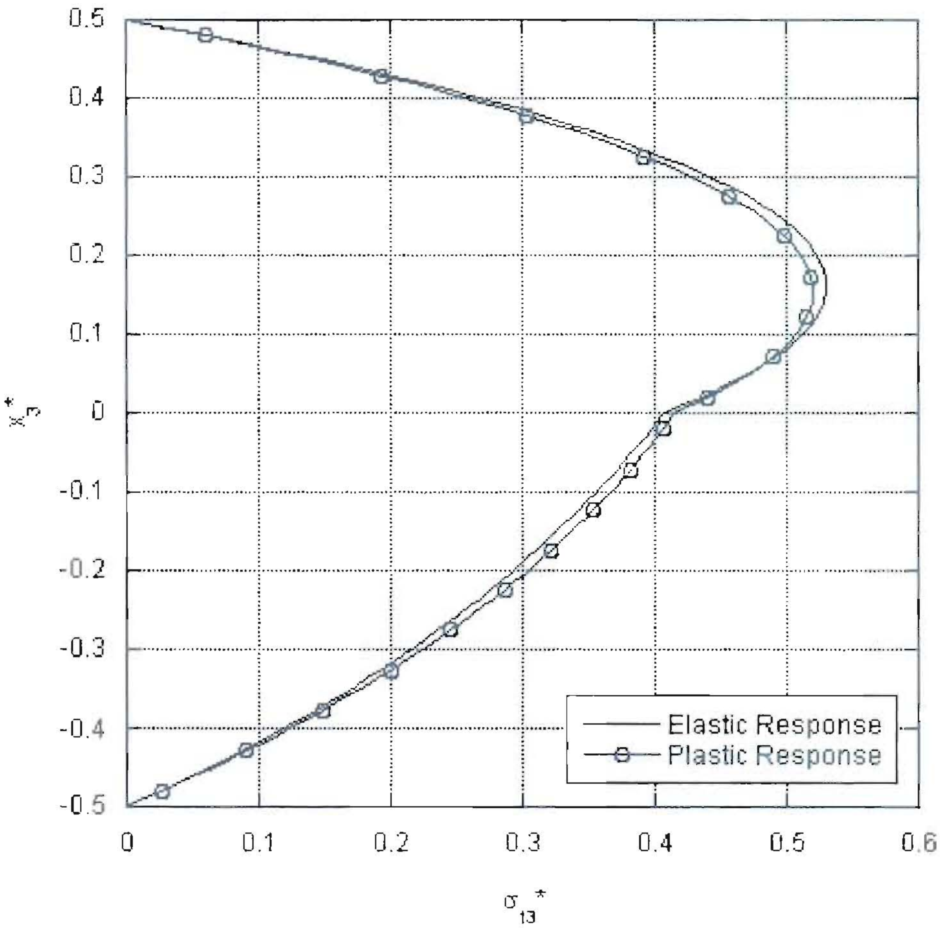

Figure 5. Distribution of σ_{13}^* through the thickness of the plate for both elastic and plastic responses.